Biochemical Interactions within a Ternary Complex of the Bacteriophage T4 Recombination Proteins uvsY and gp32 Bound to Single-Stranded DNA†

Mark A. Sweezy and Scott W. Morrical*

Department of Biochemistry, Department of Microbiology and Molecular Genetics, and Vermont Cancer Center, University of Vermont College of Medicine, Burlington, Vermont 05405

Received July 15, 1998; Revised Manuscript Received October 15, 1998

ABSTRACT: The presynaptic phase of homologous recombination requires the formation of a filament of single-stranded DNA (ssDNA) coated with a recombinase enzyme. In bacteriophage T4, at least three proteins are required for the assembly of this presynaptic filament. In addition to the T4 recombinase, uvsX protein, the T4 ssDNA binding protein (gp32), and the uvsY recombination accessory protein are also required. Here we report on a detailed analysis of a tripartite filament containing ssDNA bound by stoichiometric quantities of both uvsY and gp32, which appears to be an important intermediate in the assembly of the T4 presynaptic filament. We demonstrate that uvsY and gp32 simultaneously co-occupy the ssDNA in a noncompetitive fashion. In addition, we show that protein−protein interactions between uvsY and gp32 are not required for the assembly of this ternary complex and do not affect the affinity of uvsY for the ssDNA lattice. Finally, we demonstrate that the interaction of gp32 with the ssDNA is destabilized within this complex, in a manner which is independent of gp32−uvsY interactions. The data suggest that the uvsY protein acts to remodel the gp32−ssDNA complex via uvsY−ssDNA interactions. The implications of these findings for the mechanism of presynapsis in the T4 recombination system are discussed.

In bacteriophage T4, the assembly of a presynaptic filament is an obligatory step in the initiation of homologous genetic recombination. A presynaptic filament consists of a ssDNA[1]−protein complex that is competent to invade duplex DNA and initiate a search for homology. Genetic and biochemical studies have identified a variety of protein components that are required for the presynaptic phase of recombination in T4. These proteins include uvsX, the recA-like recombinase of T4, gp32, the T4 ssDNA binding protein or ssb, and uvsY, an accessory factor of uvsX (*1*−*8*). Current models of the T4 presynapsis are based primarily on studies of the uvsX protein's enzymatic activities and the effects of gp32 and uvsY on these activities. The reactions catalyzed by uvsX include ssDNA-dependent ATP hydrolysis, DNA strand exchange (homologous pairing and 5′ → 3′ branch migration), and initiation of recombination-dependent DNA synthesis (*1*, *5*, *8*, *9*). Common features of the current models for presynaptic filament formation include the initial coating of ssDNA by gp32 and the subsequent loading of uvsX by the uvsY accessory protein onto the gp32-coated ssDNA (*10*, *11*). However, the roles of specific macromolecular interactions in the assembly of a competent presynaptic filament remain to be elucidated.

It is well established that ssDNA binding proteins (ssbs) play key roles in the initiation of recombination. In T4, the gp32 protein binds tightly and cooperatively to ssDNA (*12*) and also exhibits specific protein−protein interactions with uvsX and uvsY (*13*, *14*). It is generally accepted that gp32 coats and stabilizes all ssDNA prior to the initiation of most DNA metabolic events in vivo. It is also likely that gp32 acts to sequester the displaced strand that is generated through the strand invasion process during DNA strand exchange (*15*). Thus, it appears that gp32 acts in both the pre- and postsynaptic phases of recombination. In the T4 in vitro system, gp32 is a required cofactor for DNA strand exchange reactions catalyzed by the uvsX recombinase (*8*). However, gp32 strongly inhibits all uvsX-catalyzed activities when present in saturating quantities with respect to ssDNA binding sites (*2*, *6*, *8*, *16*), presumably through the exclusion of uvsX from the ssDNA substrate. Due to its much greater observed affinity for ssDNA, gp32 would outcompete uvsX if a direct competition for binding sites on the ssDNA lattice exists between gp32 and uvsX (*17*). This block to uvsX-catalyzed biochemical activities can be overcome through the addition of uvsY, which acts to relieve the obstruction of uvsX−ssDNA interactions created by gp32 (*2*, *3*, *6*, *16*, *18*).

Although the uvsY protein possesses no known enzymatic activities, genetic studies have demonstrated that the uvsY protein is essential for all uvsX-dependent recombination processes in vivo (*19*−*22*). In vitro, uvsY has been shown to possess both single-stranded and double-stranded DNA binding activities (*2*, *4*, *23*). Detailed characterization of the

† This work was supported by Grant GM48847 from the National Institutes of Health. M.A.S. was supported in part by a Minority Graduate Research Fellowship from the National Science Foundation.

* To whom correspondence and reprint requests should be addressed. Telephone: (802) 656-8260. Fax: (802) 862-8229. E-mail: smorrica@zoo.uvm.edu.

[1] Abbreviations: ssDNA, single-stranded DNA; ϵDNA, etheno-modified ssDNA; ssb, ssDNA binding protein (generic); gp32 (gene 32 protein), T4 ssDNA binding protein; gp32-A, truncation of the gp32 protein consisting of amino acids 1−253; SSB, *Escherichia coli* ssDNA binding protein; RP-A, eukaryotic ssDNA binding protein; SDS, sodium dodecyl sulfate; PAGE, polyacrylamide gel electrophoresis; ssDC, single-stranded DNA cellulose.

10.1021/bi9817055 CCC: $18.00
Published on Web 12/23/1998

ssDNA binding activity of uvsY has shown it binds four nucleotide residues per uvsY monomer, a site size identical to that of uvsX, in a noncooperative manner with an intrinsic binding constant comparable to that of gp32 at physiological ionic strengths (*17*, *23*). In addition to its interactions with DNA, uvsY exhibits protein−protein interactions with itself (*11*), with gp32 (*14*), and with uvsX (*13*). The interactions of uvsY with uvsX and gp32 are thought to modulate its function and vice versa; however, the functional significance of these interactions is not well understood. Recent characterization of the homospecific uvsY−uvsY interactions demonstrated that uvsY exists predominantly as a hexamer in solution and that the uvsY hexamer is competent to bind ssDNA (*11*).

There is a growing body of evidence which suggests that uvsY and gp32 can form a ternary complex on ssDNA and that this complex is an important intermediate in the assembly of the uvsX−ssDNA presynaptic filament (*2*, *10*, *18*). To date, evidence for the existence of a ternary uvsY−gp32−ssDNA complex is indirect and based predominantly on oligonucleotide gel mobility shift patterns, partial proteolysis, and hydroxyl radical fingerprinting methods. While these methods have proven to be sufficient for demonstrating that one protein is bound to ssDNA in the presence of the other, no method used to date has unambiguously detected both proteins simultaneously bound to the ssDNA. Furthermore, essential information such as the stoichiometry and biochemical properties of the putative uvsY−gp32−ssDNA complex have yet to be determined.

In this study, we employ etheno-DNA (ϵDNA) fluorescence enhancement assays and analytical ssDNA−cellulose affinity chromatography to detect uvsY−gp32−ssDNA complexes and to characterize the effects of gp32−uvsY protein−protein interactions on the ssDNA binding properties of both proteins in the complex. To assess the significance of the gp32−uvsY interaction, we employed the gp32-A protein. This protein is a C-terminal truncation of the gp32 protein (residues 1−253) which retains the ssDNA binding properties of the native protein but does not interact with uvsY (*18*, *24*, *25*). Our results demonstrate that uvsY and gp32 do form a ternary complex on ssDNA and that the stoichiometry of binding of either protein is not affected by the presence of the heterologous protein species. In addition, we demonstrate that both proteins are in contact with the ssDNA in this complex, and that gp32−uvsY interactions are not required for the binding of uvsY to a gp32−ssDNA complex. Finally, we demonstrate that uvsY destabilizes the interaction of gp32 with ssDNA in a manner independent of protein−protein interactions. These results are discussed in the context of current models for presynapsis in the bacteriophage T4 recombination system.

EXPERIMENTAL PROCEDURES

Reagents and Buffers. All chemicals used were reagent grade and were purchased from Sigma unless otherwise noted. Aqueous solutions were prepared with deionized, glass-distilled water. All fluorescence experiments were carried out in a chloride buffer system containing 20 mM Tris-HCl (pH 7.4), 1 mM $MgCl_2$, and 50 mM NaCl, which was sterile filtered through a 0.45 μm membrane prior to being used. ssDNA−cellulose affinity chromatography buffers were prepared as follows. DC-50, DC-200, DC-600, and DC-2000 buffers contained 20 mM Tris-HCl (pH 7.4), 0.5 mM EDTA, and 10% glycerol (w/v), with either 50, 200, 600, or 2000 mM NaCl, respectively.

Proteins and Nucleic Acids. The gp32 (34 kDa), gp32-A (28 kDa; gp32 amino acid residues 1−253), and uvsY (16 kDa) proteins were purified as previously described (*23*, *26*, *27*). An estimation of protein purity was made via analysis of SDS−polyacrylamide gels stained with Coomassie Brilliant Blue. All proteins were determined to be greater than 98% homogeneous by this method. The protein concentrations were determined from the absorbance at 280 nm, using extinction coefficients calculated from the amino acid sequences according to the method of Gill and von Hipple (*28*): 41 360 M^{-1} cm^{-1} for gp32, 34 570 M^{-1} cm^{-1} for gp32-A, and 19 180 M^{-1} cm^{-1} for uvsY.

Circular single-stranded DNA from phagemid M13mp19 was isolated from purified phage particles according to published procedures (*29*). Native ssDNA concentrations were determined via the absorbance at 260 nm using a conversion factor of 33 μg/mL per absorbance unit. All DNA concentrations are expressed as micromoles of nucleotide residues per liter. Etheno modification of full-length circular M13mp19 ssDNA was performed as previously described (*23*, *30*). The integrity of the etheno-modified ssDNA (ϵDNA) was monitored via agarose gel electrophoresis; the ϵDNA ran as a single band with a slightly slower mobility than unmodified M13mp19 ssDNA circles, and no fragmentation of the ϵDNA was observed. The ϵDNA concentration was determined via phosphate analysis (*23*, *31*).

Etheno-DNA (ϵDNA) Fluorescence Enhancement Assays. All fluorescence experiments were conducted using an SLM model 8000 spectrofluorimeter, attached to an external water bath to keep the sample at a constant temperature of 25 °C. All experiments were carried out in an initial volume of 2 mL of chloride buffer, prior to the addition of titrant. The excitation and emission wavelengths were 300 and 405 nm, respectively, and the band-pass was set at 5 nm. Corrections for inner filter effects, dilution, protein fluorescence, and photobleaching of the protein fluorescence signal were made as previously described (*23*). No correction was made for photobleaching of the ϵDNA lattice, as no photobleaching was observed in control experiments. To maintain a constant ionic strength, the NaCl concentration in protein storage buffers was adjusted to 50 mM prior to their addition to binding reaction mixtures. ϵDNA challenge experiments were performed by incubating 5 μM unmodified ssM13mp19 ssDNA with slightly subsaturating amounts of gp32 (0.5 μM) and/or uvsY (1.1 μM) in chloride buffer for 5 min at 25 °C. The sample fluorescence was monitored at 1 min intervals to ensure complete equilibration, i.e., no further signal change had occurred. Once these complexes were formed, 5 μM ϵDNA was added to the reaction mixture and the change in ϵDNA fluorescence was monitored over time. Corrections for fluorescence and photobleaching of the protein were made by omitting the addition of ϵDNA and subtracting the resulting fluorescence signal from the experimental values. Experiments in which the unmodified M13mp19 ssDNA was omitted provided a reference for the maximal ϵDNA fluorescence enhancement signal and the rate of fluorescence change in the reactions of free protein with ϵDNA.

Analytical ssDNA−Cellulose Affinity Chromatography. The ssDNA−cellulose matrix (ssDC) was prepared as previously described (*32*). The matrix was washed extensively in 2.0 M NaCl and resuspended in an equal volume of DC-50. Estimations of ssDNA that was accessible to protein were made by treating an aliquot of the matrix with DNase I (Sigma) (*12*) and quantifying the released nucleotides via phosphate analysis (*23*, *31*). This method indicated that the concentration of immobilized ssDNA that was accessible to protein was 320 μM (nucleotides). Binding reactions were performed in the batch mode in plastic 1.5 mL microcentrifuge tubes, containing 0.5 mL (bed volume) of ssDC matrix incubated with a 2-fold molar excess of gp32, gp32-A, and/or uvsY protein (with respect to protein-accessible ssDNA binding sites) in a total volume of 1.0 mL of DC-50 buffer. Binding reactions were carried out for 1 h at 4 °C, with gentle agitation to keep the matrix in suspension. The matrix was then allowed to settle, and the supernatant was removed. The quantity of protein bound to the matrix was determined through A_{280} measurements of the unbound protein left in the supernatant after the binding reaction, using extinction coefficients for the three proteins listed above. In ternary reaction mixtures containing either gp32 or gp32-A plus uvsY, the proteins were added to the matrix sequentially with the gp32 species added first and the mixtures incubated for 1 h at 4 °C, and then uvsY was added and incubation continued for 1 h. In all experiments, following incubation the protein-bound matrixes were poured into 1.0 mL columns (bed volume of 0.5 mL) and washed under gravity with 5 column volumes of DC-50. These columns were then step eluted with 5 column volumes each of DC-200, DC-600, and DC-2000. All elutions were performed under gravity, and 0.5 mL fractions were collected. To assess the extent of DNA leaching from the matrixes during the elution, a comparison of the A_{260}:A_{280} ratios of the protein loaded and the column eluants was made. Analysis of the elution profiles was carried out via SDS−PAGE and subsequent staining with Coomassie Brilliant Blue.

RESULTS

gp32 Binds Stoichiometrically to a uvsY-Saturated ϵDNA Lattice. In an effort to assess the coincidental interactions of uvsY and gp32 with ssDNA, we exploited an inherent difference in the enhancement of ϵDNA fluorescence produced through the binding of these proteins. Upon saturation of ϵDNA, the gp32 protein generates an approximately 2-fold enhancement of the intrinsic ϵDNA fluorescence. This enhancement signal has been attributed to the disruption of base stacking interactions upon binding of gp32 to the ϵDNA lattice (*33*, *34*). As previously reported (*23*), under conditions of relatively low ionic strength, the uvsY protein produces a 4−6-fold enhancement of ϵDNA fluorescence. While the underlying mechanism for this phenomenon has not been characterized, one possible explanation is through the greater isolation of individual fluorescent bases in the uvsY−ϵDNA complex.

To ascertain which level of fluorescence enhancement would prevail in the presence of both proteins, ϵDNA was incubated with saturating amounts of uvsY and the fluorescence signal was monitored (Figure 1A). An excess of gp32 or gp32-A was then added to this complex, and the change in fluorescence was monitored. This experiment was then repeated, reversing the order of addition of the proteins. The data indicate that the prevailing ϵDNA fluorescence enhancement signal in the presence of both uvsY and either gp32 or gp32-A is the 2-fold enhancement characteristic of the gp32-bound form. However, it is not possible in this experiment to ascertain whether this signal results from the displacement of uvsY from ϵDNA by gp32 or from a gp32-induced attenuation of the uvsY−ϵDNA fluorescence signal. On the

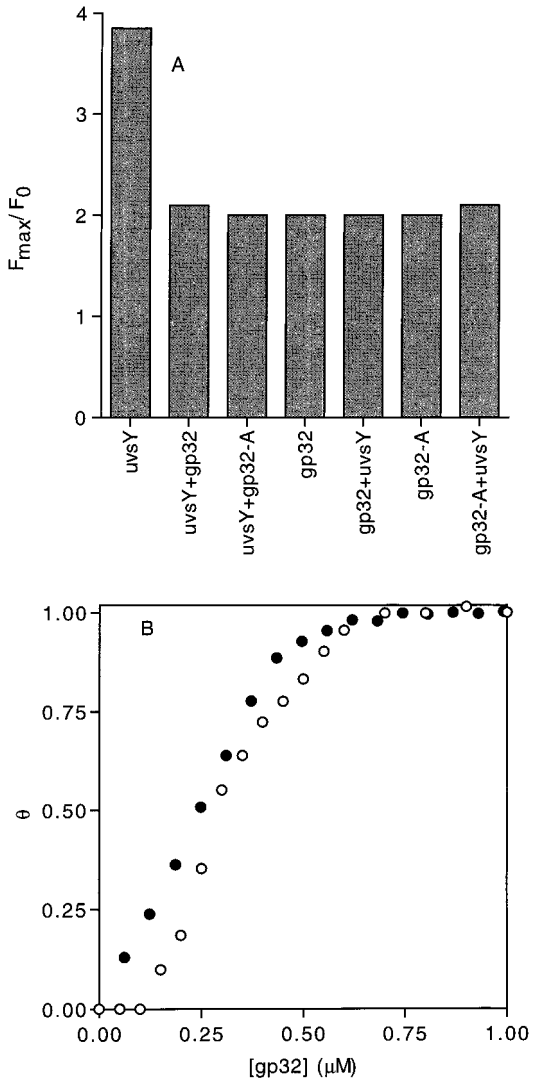

FIGURE 1: Analysis of the ϵDNA fluorescence enhancement properties of gp32−uvsY−ϵDNA tripartite reactions. (A) Maximum enhancement of ϵDNA fluorescence at saturation (F_{max}/F_0), for uvsY, gp32, and gp32-A protein species, and combinations thereof as indicated in the bar graph labels. Binding reactions were conducted in a chloride buffer system (see Experimental Procedures) supplemented with 50 mM NaCl. The ϵDNA concentration was 5 μM in all experiments; the uvsY concentration was 2 μM when it was present, and the gp32 and gp32-A concentrations were 1 μM when they were present. In reaction mixtures containing two protein species, the effect of the order of protein addition to the ϵDNA fluorescence enhancement was also tested. The initial protein added is listed first on the bar graph label. (B) Forward titration of gp32 onto uvsY-saturated ϵDNA, monitoring the decrease in ϵDNA fluorescence enhancement. Experimental conditions were as described for panel A. gp32 was titered in a stepwise fashion onto 5 μM ϵDNA preincubated with 2 μM uvsY protein (○). The data are plotted in terms of fractional saturation of the ϵDNA lattice; an otherwise identical titration of gp32 onto naked ϵDNA is overlayed for purposes of comparison (●).

basis of these results, we sought a more detailed analysis of the interaction of gp32 with ϵDNA in the presence of uvsY.

Forward titrations of gp32 onto a pre-existing uvsY−ϵDNA complex were conducted to assess the binding properties of gp32 on a uvsY-saturated lattice. The decrease in ϵDNA fluorescence was monitored with each addition of gp32 to the binding reaction mixture. If we assume that the point in the titration at which there is no further change in fluorescence with increasing gp32 concentration represents saturation of the lattice with gp32, these data can be plotted in terms of fractional saturation of the uvsY−ϵDNA lattice with gp32 (Figure 1B). For the purpose of comparison, these data are overlaid with a plot of a forward titration of gp32 onto naked ϵDNA under identical buffer conditions. The data reveal two pertinent features. First, the stoichiometry of gp32 binding (binding site size $n = 10$) is not affected by the presence of saturating amounts of uvsY, as evidenced by the lack of a significant shift in the titration end point with or without uvsY (Figure 1B). Second, the uvsY-enhanced ϵDNA fluorescence signal is resistant to low concentrations of gp32, as evidenced by the lag zones in Figure 1B. One possible explanation for this is that a large amount of gp32 is required to either displace uvsY or alter the conformation of the uvsY-coated lattice, allowing gp32−ϵDNA binding; an alternative explanation is that the binding of small amounts of gp32 does not ameliorate the hyperenhancement of ϵDNA fluorescence produced by the uvsY protein. Again we must emphasize that while these forward titrations are useful in describing the interaction of gp32 with ϵDNA in the presence of saturating amounts of uvsY, a different approach is required to determine the fate of uvsY in these reactions.

uvsY and gp32 Form a Stoichiometric Cofilament on ssDNA. To obtain information on the status of both gp32 and uvsY in the tripartite binding reactions, fluorescence studies were performed using unmodified M13mp19 ssDNA and slightly subsaturating (0.9 times saturating with respect to binding sites) amounts of either gp32, uvsY, or both proteins combined. These reactions were then challenged with an equimolar amount, with respect to unmodified ssDNA, of ϵDNA, and the fluorescence change was monitored over time as an indicator of the unbound protein available to bind to the ϵDNA lattice (Figure 2). As a control, identical reactions were performed in the absence of unmodified ssDNA. The data in these control experiments (Figure 2, black symbols) represent the kinetics of stoichiometric binding of uvsY, gp32, or both to the ϵDNA lattice. In each control reaction, the maximal ϵDNA fluorescence enhancement signal was obtained by the first time point (10 s after ϵDNA addition), indicating that in the absence of preincubation of proteins with unmodified ssDNA, the formation of protein−ϵDNA complexes is very rapid in all cases. (Note that the final fluorescence signals obtained in the control reactions match the relative fluorescence enhancement levels depicted for the various reactions in Figure 1A.)

In the experimental reactions (Figure 2, white symbols), where complexes were preassembled on unmodified ssDNA, a net transfer of protein to the ϵDNA lattice upon ϵDNA addition is expected with time, since both uvsY and gp32 exhibit higher intrinsic affinities for the etheno-modified form of polynucleotides at equilibrium (*23*, *35*). Therefore, the fluorescence signal should increase with time following

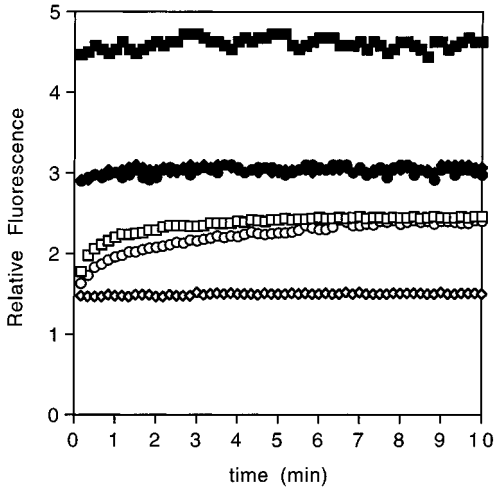

FIGURE 2: ϵDNA challenge of preformed complexes containing unmodified ssDNA with uvsY and/or gp32. (White symbols) Protein−ssDNA complexes were preassembled in chloride buffer as described in Experimental Procedures; then ϵDNA was added at time zero to begin the challenge reaction, and the increase in ϵDNA fluorescence was monitored with time. Preincubation mixtures contained final concentrations of 5 μM unmodified ssDNA, with (□) 1.1 μM uvsY, (◇) 0.5 μM gp32, or (○) 0.5 μM gp32 and 1.1 μM uvsY. Both protein concentrations represent 0.9-fold saturation with respect to binding sites on the ssDNA. Following preincubation of the protein−ssDNA mixtures, 5 μM (final concentration) ϵDNA was added to each via a small aliquot. (Black symbols) The unmodified ssDNA was omitted, and 5 μM ϵDNA (final concentration) was added at time zero to solutions containing either (■) 1.1 μM uvsY, (◆) 0.5 μM gp32, or (●) both 1.1 μM uvsY and 0.5 μM gp32.

ϵDNA addition to the preincubated protein−ssDNA complexes. A rapid jump in fluorescence would be indicative of unbound protein present in the protein−ssDNA preincubation mixture (e.g., uvsY or gp32 displaced from ssDNA in the tripartite reactions), consistent with the rapid kinetics seen in control experiments with both proteins (Figure 2, black symbols). Alternatively, sequestration of both uvsY and gp32 within a ternary uvsY−gp32−ssDNA complex may be expected to retard the rate of protein transfer to ϵDNA.

Results in Figure 2 (white symbols) show that in each case (uvsY, gp32, or uvsY and gp32) fluorescence did not increase rapidly upon addition of ϵDNA to the preincubated protein−ssDNA mixture. In the case of the preformed gp32−ssDNA complex, virtually no increase in ϵDNA fluorescence was observed over the entire time course of the experiment (Figure 2, ◇), indicating a very slow rate of transfer of gp32 between polynucleotides, consistent with the high $K\omega$ and low k_{off} observed for gp32−ssDNA at the relatively low salt concentration used in this experiment (*36*). In the case of the preformed uvsY−ssDNA complex, a time-dependent increase in ϵDNA fluorescence was observed (Figure 2, □); however, the rate of fluorescence increase was dramatically slower than the immediate jump seen in the absence of ssDNA (■). In this experiment, the uvsY−ϵDNA fluorescence signal appears to approach a plateau value that is well below the signal seen for uvsY−ϵDNA in the absence of unmodified ssDNA, with an estimated half-time of 30−45 s (Figure 2, □). The plateau fluorescence value is assumed to represent the equilibrium distribution of uvsY between the ϵDNA and unmodified ssDNA lattices under these experimental conditions. The slow kinetics of the fluorescence increase indicates that all of the uvsY was bound to

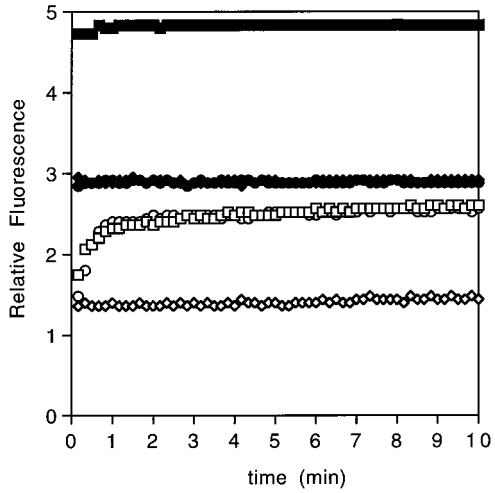

FIGURE 3: ϵDNA challenge of preformed complexes containing unmodified ssDNA with uvsY and/or gp32-A. Reactions were identical to those in Figure 2 except that gp32-A was substituted for gp32. (White symbols) Preincubation mixtures contained final concentrations of 5 μM unmodified ssDNA, with (□) 1.1 μM uvsY, (◇) 0.5 μM gp32-A, or (○) 0.5 μM gp32-A and 1.1 μM uvsY. Challenge reactions were started by the addition of 5 μM ϵDNA (final concentration) at time zero, and the increase in ϵDNA fluorescence was monitored with time. (Black symbols) The unmodified ssDNA was omitted, and 5 μM ϵDNA (final concentration) was added at time zero to solutions containing either (■) 1.1 μM uvsY, (◆) 0.5 μM gp32-A, or (●) both 0.5 μM gp32-A and 1.1 μM uvsY.

unmodified ssDNA prior to ϵDNA addition and suggests that dissociation of the preformed uvsY−ssDNA complex is the rate-limiting step in the transfer of uvsY to the ϵDNA lattice.

In the reaction wherein uvsY and gp32 were both preincubated with unmodified ssDNA (Figure 2, ○), we also observed a relatively slow, time-dependent increase in ϵDNA fluorescence upon addition of the ϵDNA. The absence of a rapid fluorescence increase indicates that both proteins were bound stoichiometrically to the ssDNA prior to ϵDNA addition, providing compelling evidence for the existence of a ternary uvsY−gp32−ssDNA complex. Another interesting feature of this reaction is the reduction of the initial rate of ϵDNA fluorescence enhancement in the tripartite reaction when compared to that of the reaction whose mixture contains only uvsY−ssDNA (Figure 2). We assume that the fluorescence increase in this experiment represents the transfer of uvsY protein from the uvsY−gp32−ssDNA ternary complex to the ϵDNA, since (1) the fluorescence signal in this experiment (○) appears to approach the identical plateau value seen in the experiment with uvsY−ssDNA (□) and (2) the rate of gp32 transfer from gp32−ssDNA to ϵDNA (◇) is negligible. Given the validity of this assumption, then the data imply that gp32 reduces the rate of uvsY dissociation from the ternary complex without affecting the final equilibrium distribution of uvsY between the ternary complex and ϵDNA. However, we must emphasize that at present we cannot prove the validity of our assumption, so the possibility remains that the fluorescence increase seen in the tripartite reaction represents the transfer of both proteins or of gp32 alone. The effect of gp32−uvsY interactions on the affinity of uvsY for the ssDNA lattice is addressed independently below (see Figure 4).

Both gp32 and uvsY Are in Direct Contact with ssDNA. To address the issue of whether both proteins contact the

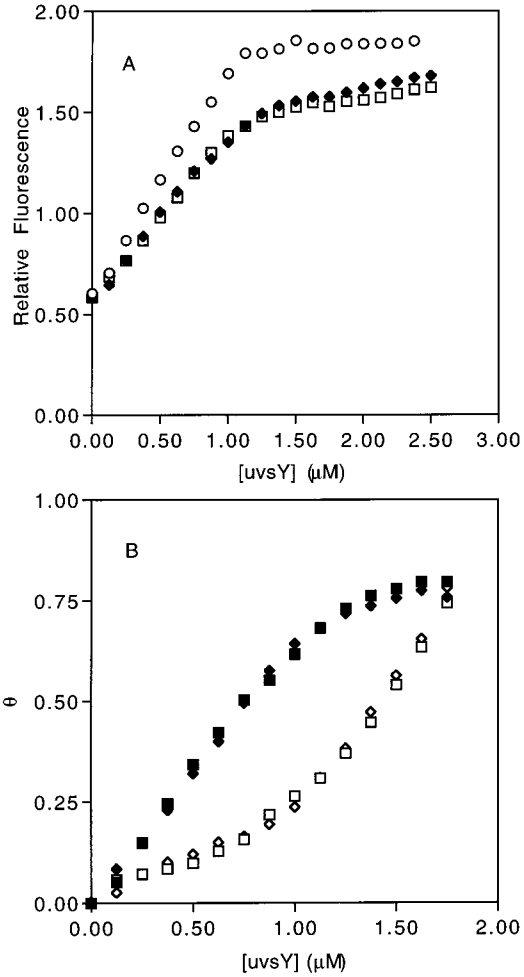

FIGURE 4: Competition titrations of uvsY protein onto ϵDNA and ssDNA lattices or onto ϵDNA and gp32-saturated ssDNA lattices. Reaction conditions and data correction procedures are described in Experimental Procedures and in the text. (A) ϵDNA fluorescence was monitored while uvsY was titered into solutions containing either (○) 5 μM ϵDNA alone, (◆) 5 μM ϵDNA and 5 μM unmodified ssDNA, or (□) 5 μM ϵDNA and 5 μM unmodified ssDNA presaturated with 0.5 μM gp32. (B) The data in panel A were replotted in terms of fractional saturation of the ϵDNA (black symbols) and unmodified (white symbols) lattices, assuming stoichiometric binding of uvsY to all of the experimental lattices in the chloride buffer system used here. ◆ and ◇ denote the fractional saturations of uvsY on the ϵDNA and unmodified ssDNA lattices, respectively, in the ϵDNA and ssDNA competition titration. ■ and □ denote the fractional saturations of uvsY on the ϵDNA and gp32-saturated unmodified ssDNA lattices, respectively, in the ϵDNA and gp32−ssDNA competition titration. Fractional saturation of the unmodified lattice (with or without gp32) was determined as the difference between the level of saturation of the ϵDNA lattice in a control reaction mixture containing no competitor DNA and the level of saturation of the ϵDNA lattice in the competition reaction.

DNA in the ternary complex, we utilized the gp32-A truncation. The gp32-A protein binds cooperatively to ssDNA with an affinity similar to that of native gp32 but does not interact with uvsY (*18*, *24*, *25*). In the experiment described in Figure 3, both gp32-A and uvsY were incubated at slightly subsaturating concentrations with M13mp19 ssDNA and then challenged with an equimolar amount of ϵDNA. Fluorescence was monitored over time as described in the legend of Figure 2. The results indicate that both uvsY and gp32-A bind stoichiometrically to the unmodified ssDNA lattice, since there is no rapid increase in ϵDNA fluorescence observed

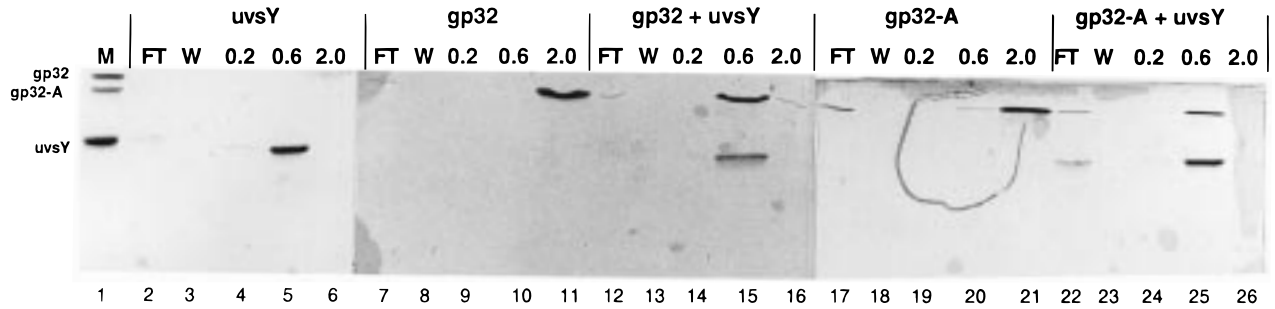

FIGURE 5: SDS−PAGE analysis of ssDNA−cellulose affinity chromatography experiments. Results are also summarized in Table 1. Reaction and electrophoresis conditions are described in Experimental Procedures. The samples shown represent 10 μL aliquots from each fraction. Lane 1 contains markers (M) for gp32, gp32-A, and uvsY proteins as indicated. Other labels denote for each column flow-through (FT), wash (W), 0.2 M NaCl (0.2), 0.6 M NaCl (0.6), and 2.0 M NaCl (2.0) fractions, respectively: lanes 2−6, elution profile of uvsY protein alone; lanes 7−11, elution profile of gp32 alone; lanes 12−16, elution profiles of uvsY and gp32 bound simultaneously; lanes 17−21, elution profile of gp32-A alone; and lanes 22−26, elution profiles of uvsY and gp32-A bound simultaneously.

in the tripartite reaction (Figure 3, ○). In contrast, control experiments lacking ssDNA showed immediate jumps in fluorescence upon ϵDNA addition to either uvsY, gp32-A, or both (Figure 3, black symbols). Note however that the apparent stabilization of uvsY within the ternary complex observed with full-length gp32 (Figure 2) is not seen with gp32-A, since the kinetics of ϵDNA fluorescence increase is identical in the uvsY−(gp32-A)−ssDNA and uvsY−ssDNA reactions (Figure 3). In the reaction with preincubated (gp32-A)−ssDNA, no significant transfer of gp32-A to the ϵDNA was observed over the time course of the experiment, similar to results obtained with full-length gp32 (see Figure 2).

The results in Figure 3 indicate that the uvsY protein is capable of interacting stoichiometrically with (gp32-A)−ssDNA complexes in the absence of uvsY−gp32 protein−protein interactions; therefore, both proteins in the complex must make contact with the ssDNA. This lack of dependency on protein−protein interactions between uvsY and gp32 is in apparent contradiction with previous studies (*18*) in which gel mobility shift and protein cross-linking methods were used. Jiang et al. (*18*) failed to detect uvsY−(gp32-A)−oligonucleotide complexes by gel mobility shift and concluded uvsY is excluded from (gp32-A)−ssDNA. Alternatively, it is possible that the uvsY−(gp32-A)−ssDNA has a gel mobility very similar to that of uvsY−ssDNA or (gp32-A)−ssDNA, or that the ternary complex may be unstable under the conditions required for electrophoresis. The other evidence cited by Jiang et al. for a requirement of protein−protein interactions between uvsY and gp32 comes from protein cross-linking studies (*18*). These experiments showed that cross-linking of gp32 and uvsY is enhanced in the presence of ssDNA and that this enhancement, as well as the quantity of cross-linked product, is reduced when gp32-A is substituted for gp32. These results were interpreted to imply that uvsY was excluded from the ssDNA−(gp32-A) complex (*18*). An alternative explanation is that the absence of direct protein−protein interactions within the (gp32-A)−uvsY−ssDNA complex reduces the efficiency of the cross-linking reaction.

gp32−uvsY Interactions Do Not Affect the Affinity of uvsY for ssDNA. One possible function of gp32−uvsY protein−protein interactions is to direct uvsY and subsequently uvsX assembly onto the proper gp32-coated ssDNA substrate in vivo. In this model, uvsY might be expected to show enhanced affinity for gp32-coated versus naked ssDNA. We tested this hypothesis by measuring the relative abilities of ssDNA and gp32−ssDNA to perturb the equilibrium binding of uvsY to ϵDNA.

Since there is essentially no transfer of gp32 from unmodified ssDNA to ϵDNA on the time scale shown in Figure 2, we were able to perform competition titrations which allow us to compare the affinity of uvsY for gp32-coated and naked ssDNA lattices (Figure 4). As previously reported (*23*), this type of experiment has shown that uvsY has a 2−6-fold greater affinity for ϵDNA than for unmodified ssDNA. Here we titered uvsY into a reaction mixture containing either ϵDNA alone, ϵDNA and ssDNA, or ϵDNA and preformed gp32−ssDNA (Figure 4). As shown in Figure 4A, the presence of unmodified ssDNA (with or without gp32), equimolar with respect to ϵDNA, causes a moderate rightward shift in the uvsY−ϵDNA titration curve as detected by ϵDNA fluorescence enhancement. The degree of the curve shift is nearly identical in the presence and absence of gp32. When these data are replotted as a comparison of the fractional saturation of the modified and unmodified substrates (Figure 4B), we observe a significant difference in the affinity of uvsY for the ϵDNA and unmodified ssDNA lattices with preference for the former, consistent with previous results (*23*). However, the affinity of uvsY for the naked and gp32-coated ssDNA lattices is essentially identical (Figure 4B). Under these conditions, uvsY displays a 2−6-fold greater affinity for the ϵDNA lattice than either the naked or gp32-coated ssDNA lattice. Thus, as suggested by the data in Figure 2, the presence of gp32 on ssDNA does not affect uvsY−ssDNA equilibrium binding properties, although a kinetic effect of gp32−uvsY interactions on uvsY's dissociation from the ternary complex appears to be evident (see Figures 2 and 3).

The Interaction of uvsY with ssDNA Destabilizes gp32−ssDNA Interactions. In an effort to better characterize the effect of gp32−uvsY interactions on the stability of the ternary complex, we employed a ssDNA−cellulose affinity chromatography assay (Figure 5 and Table 1). In these experiments, an excess, with respect to protein-accessible binding sites on ssDNA (see Experimental Procedures), of either gp32, gp32-A, uvsY, gp32 and uvsY, or gp32-A and uvsY was incubated with 0.5 mL of ssDNA−cellulose at 4 °C with gentle agitation. In reaction mixtures containing uvsY and either gp32 or gp32-A, the proteins were bound sequentially, with the gp32 species being loaded first. Once the ssDNA−cellulose matrix was saturated, the slurry was

Table 1: Summary of ssDNA−Cellulose Affinity Chromatography Experiments[a]

column number	protein loaded[b]	quantity bound[c] (mg)	elution step [NaCl][d] (M)	A_{260}:A_{280} ratio, protein loaded:eluted[e]
1	uvsY	0.62	0.6	1.04
2	gp32	0.57	2.0	1.03
3	gp32	0.56	0.6	0.98
	uvsY	0.64	0.6	
4	gp32-A	0.52	2.0	1.02
5	gp32-A	0.50	0.6	1.02
	uvsY	0.61	0.6	

[a] Experiments were performed batch-style as described in Experimental Procedures. [b] For experiments involving two protein species (columns 3 and 5), the proteins were loaded sequentially, with the gp32 sp. loaded prior to uvsY, as described in Experimental Procedures. [c] The amount of protein bound to the matrix was determined from the decrease in absorbance at 280 nm following sample equilibration with matrix, as described in Experimental Procedures. For columns 3 and 5, the amounts of gp32 sp. and uvsY bound were determined separately for each stepwise addition and equilibration of protein. [d] Concentration of NaCl required to elute each protein species from the equilibrated ssDNA−cellulose matrix. [e] A_{260}:A_{280} ratios for protein samples loaded onto vs eluted from each ssDNA−cellulose column; control for ssDNA leaching off of ssDNA−cellulose. Since all values were within experimental error of unity, we conclude that significant ssDNA leaching did not occur and cannot account for changes in protein elution profiles.

poured into 1.0 mL glass columns and washed extensively with loading buffer containing 0.05 M NaCl. In all cases, the amount of each protein retained on the column was sufficient to saturate greater than 85% of the protein-accessible binding sites determined by the nuclease digestion method (Table 1; see Experimental Procedures). The columns were then step eluted with loading buffer supplemented with 0.2, 0.6, and 2.0 M NaCl, respectively. Results are shown in Figure 5 and summarized in Table 1. The absorbance ratios (A_{260}:A_{280}) of the eluted proteins were compared to those of the proteins loaded as a control for DNA leaching from the ssDNA−cellulose matrix. In all cases, we found that the A_{260}:A_{280} ratios were identical for the loaded and eluted samples (Table 1); therefore, leaching of ssDNA from the columns during the experiments was judged to be negligible. The data in Table 1 show that in the ternary reactions (uvsY and gp32 or uvsY and gp32-A), the presence of a heterologous protein species did not alter the capacity of the ssDNA−cellulose for either protein. This provides further support for the assembly of a stoichiometric tripartite complex independent of interactions between gp32 and uvsY (Table 1). SDS−PAGE analysis of column elution profiles is presented in Figure 5. As expected, the uvsY eluted at 0.6 M NaCl and both gp32 and gp32-A eluted at 2.0 M NaCl (*23*, *26*, *27*). Interestingly, in experiments with either gp32 and uvsY or gp32-A and uvsY, essentially all the protein was eluted in the 0.6 M NaCl step. These data indicate that the uvsY protein destabilizes the gp32−ssDNA interaction and that this destabilization is independent of protein−protein interactions between gp32 and uvsY.

DISCUSSION

Our studies of uvsY−gp32−ssDNA ternary complexes have revealed the following. (1) The T4 uvsY and gp32 proteins are capable of co-occupying ssDNA at their normal stoichiometries of binding. This finding demonstrates that uvsY and gp32 do not compete directly for binding sites

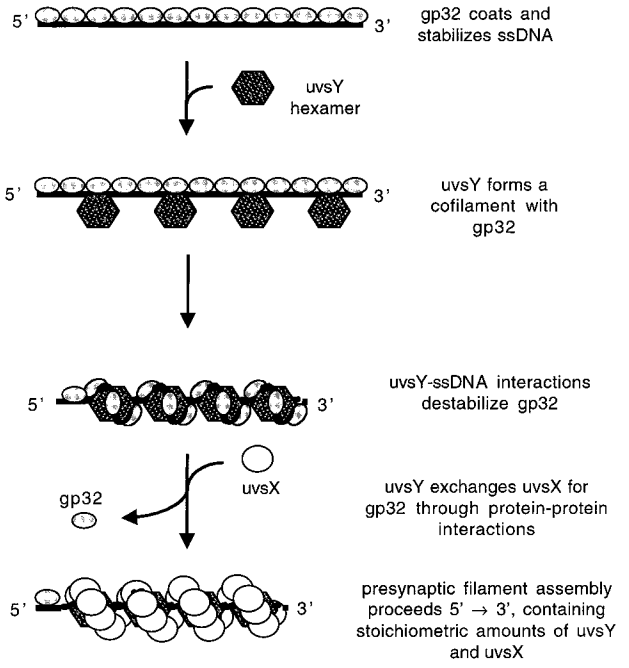

FIGURE 6: Model for the role of a stoichiometric uvsY−gp32−ssDNA cofilament in the assembly of a mature uvsX−uvsY−ssDNA presynaptic filament. The uvsY protein exists predominantly as a hexamer in solution (*11*), and the hexamer is able to bind gp32-coated ssDNA in a noncompetitive fashion via uvsY−ssDNA contacts. This results in a conformational change in the ssDNA (shown here as wrapping of the ssDNA around uvsY hexamers) which destabilizes the gp32−ssDNA interaction. Then through protein−protein interactions, uvsY conducts a direct exchange of uvsX for gp32, allowing the nucleation and assembly of the presynaptic filament. Stoichiometric quantities of uvsY protein have been proposed to remain bound to the presynaptic filament, thereby stabilizing the uvsX−ssDNA interaction (*10*). See the Discussion for details.

and thus do not form isolated patches on ssDNA, but rather must form an integrated "cofilament" type of structure (see Figure 6). (2) The formation of the uvsY−gp32−ssDNA ternary complex does not require uvsY−gp32 protein−protein interactions, but rather involves direct interactions of both proteins with ssDNA. (3) The interaction of uvsY with ssDNA destabilizes gp32−ssDNA interactions without displacing gp32 from the ssDNA. The observed destabilization of gp32−ssDNA interactions does not require uvsY−gp32 protein−protein interactions. These features of uvsY−gp32−ssDNA ternary interactions are incorporated in a new model of T4 presynaptic filament formation shown in Figure 6.

Biochemical and molecular characterization of uvsY interactions with ssDNA, gp32−ssDNA, and uvsX−ssDNA complexes has led to current models in which a uvsY−gp32−ssDNA ternary complex is a key intermediate in T4 presynaptic filament formation (*2*−*4*, *10*, *11*, *18*, *23*). However, prior to this study there was no direct evidence that uvsY and gp32 could co-occupy ssDNA without competing for binding sites. Using ϵDNA fluorescence enhancement and ssDNA−cellulose affinity methods, we have now provided substantial evidence that uvsY and gp32 co-occupy ssDNA stoichiometrically at saturation, leading to an integrated nucleoprotein cofilament (Figure 6) containing approximately two uvsY monomers per gp32 monomer or three gp32 monomers per uvsY hexamer, consistent with the approximately 2-fold larger binding site size of gp32

versus uvsY on ssDNA. A further intriguing observation is that uvsY binding destabilizes gp32−ssDNA interactions, as evidenced by the increased sensitivity of the complex to disruption by salt (Figure 5). Most surprising of all is that this destabilization occurs equally well with gp32-A, the truncated form of gp32 lacking protein−protein interactions with uvsY. Therefore, uvsY clearly affects the destabilization of gp32 sp.−ssDNA complexes by altering the ssDNA conformation within a ternary uvsY−(gp32 sp.)−ssDNA complex.

Two important clues about the mechanism of ssDNA conformational change and gp32−ssDNA destabilization induced by uvsY are as follows. (1) uvsY's intrinsic affinity for ssDNA matches or exceeds that of gp32 at physiological ionic strengths (*23*). Thus, gp32's only stability advantage on ssDNA resides in its high cooperativity of binding, suggesting that the key to destabilizing gp32−ssDNA lies in neutralizing its cooperativity. In fact, our ssDNA−cellulose affinity chromatography data support the notion that the cooperativity parameter of gp32 may be reduced upon the addition of uvsY. This follows from the fact that gp32− and uvsY−ssDNA interactions within the gp32−uvsY−ssDNA ternary complex exhibit similar salt stabilities (Figure 5 and Table 1), consistent with their similar intrinsic affinity (*K*) values (*23*). Thus, the weaker interaction of gp32 with ssDNA observed in the presence or absence of uvsY may reflect a selective decrease in the cooperativity (ω) parameter of gp32−ssDNA binding, although we cannot rule out an effect of uvsY on gp32's *K* value as well. (2) uvsY exists predominantly as a hexamer in solution and binds to ssDNA as a hexamer (*11*). The hexameric structure of uvsY potentially provides multiple binding sites for ssDNA (as well as gp32 and uvsX) per binding unit of uvsY. Thus, uvsY hexamers may have the ability to wrap the ssDNA as previously proposed (*11*). As diagrammed in Figure 6, remodeling of gp32−ssDNA by wrapping the ssDNA around a uvsY hexamer is one way to disrupt the cooperativity of gp32 binding, since this structural distortion would be expected to strain interactions between neighboring gp32 molecules. The fact that both gp32− and (gp32-A)−ssDNA complexes are destabilized by uvsY indicates that destabilization is mediated solely by uvsY−ssDNA interactions, supporting the notion that wrapping or other structural distortions of the polynucleotide are responsible for the uvsY-induced destabilization of gp32 sp.−ssDNA interactions.

Given that uvsY−ssDNA interactions are sufficient for formation of the uvsY−gp32−ssDNA ternary complex and for destabilization of gp32−ssDNA interactions, what may be the role of uvsY−gp32 protein−protein interactions in T4 recombination? As suggested by the data in Figures 2 and 3, uvsY−gp32 interactions appear to decrease the rate of dissociation of uvsY from the ternary complex, though the functional significance is unclear since this apparent stabilization is strictly a kinetic, not thermodynamic, effect (see Figure 4). Previous work suggests that uvsY−gp32 interactions may be important for the synergistic stimulation of uvsX enzymatic activities by uvsY and gp32, first reported by Yonesaki and Minagawa (*2*), since an N-terminal fragment of uvsY protein which binds to ssDNA but lacks interactions with gp32 and uvsX does not support the synergism seen with wild-type uvsY (*16*).[2] In terms of mechanism, one possibility is that uvsY−gp32 interactions play a role in the final displacement of gp32 from the ssDNA upon addition of the uvsX recombinase. It may be envisioned that uvsY conducts a direct exchange of gp32 for uvsX within the filament via protein−protein interactions. At the same time, uvsY may maintain the ssDNA in a conformation which favors uvsX binding and destabilizes gp32 binding, providing uvsX a thermodynamic advantage over gp32 in competition for ssDNA binding sites (Figure 6).

On the basis of work in several laboratories, Morrical and Alberts (*3*) proposed that the uvsY protein plays a dual role in presynapsis: a *nucleation* role, in which uvsY at low binding densities provides initiation sites for uvsX−ssDNA filament formation, which are then free to propagate along the ssDNA while displacing gp32; and also a *stabilization* role, in which uvsY at higher binding densities interacts stoichiometrically with uvsX−ssDNA, stabilizing these filaments against displacement by gp32 or disruption by high salt concentrations. While this study has focused on the stoichiometric interactions of uvsY with gp32−ssDNA, conditions in which optimal enhancements of uvsX activities are observed in vitro, our results are in no way inconsistent with a nucleation activity of uvsY. As discussed previously (*11, 23*), the lack of cooperativity in uvsY−ssDNA interactions suggests that at low binding densities, individual uvsY hexamers could interact with and destabilize gp32−ssDNA complexes at isolated sites, providing recruitment and nucleation points for uvsX. It is important to note that nucleation of presynaptic filaments may be the predominant biological function of uvsY, since this protein appears to be less abundant than either gp32 or uvsX in T4-infected *Escherichia coli* cells (*37*).

The T4 uvsY protein is the first and best-characterized example of a recombination accessory protein involved in the assembly of presynaptic filaments. Recent work with bacterial and eukaryotic recombination systems indicates that uvsY-like functions are highly conserved. The RecO and RecR proteins of *E. coli* have been shown to promote the assembly of the RecA recombinase onto pre-existing SSB-ssDNA (*38*−*40*). Likewise, both the Rad52 protein and Rad55/Rad57 heterodimer of *Saccharomyces cerevisiae* appear to perform a similar function in promoting Rad51 recombinase assembly onto RP-A-saturated ssDNA (*41*−*46*). These observations lead to the notion that there is general class of proteins which functions in the loading of a recombinase onto ssb-bound ssDNA and the stabilization of a presynaptic filament once it is formed. We are currently attempting to determine the detailed biochemical mechanism by which the uvsY protein carries out these activities in the bacteriophage T4 recombination system, and thus, we are hopeful that this will provide insight into the strategies used in many organisms to promote homologous recombination.

[2] Interestingly, the N-terminal uvsY fragment, though a relatively weak ssDNA binder compared to the wild type, still provides significant stimulation of uvsX activities, including ssDNA-dependent ATP hydrolysis and DNA strand exchange at elevated gp32 and salt concentrations, where these in vitro reactions are normally codependent on uvsX and uvsY (*16*). These observations provide further evidence for the central role played by uvsY−ssDNA interactions in promoting the formation of active uvsX−ssDNA presynaptic filaments.

ACKNOWLEDGMENT

We thank Dr. David P. Giedroc of Texas A&M University (College Station, TX) for the gift of an overexpressing strain of the gp32-A protein species. We also thank David Yassa and Yujie Ma of this laboratory for their technical assistance, as well as all other members of the Morrical laboratory for their comments and suggestions.

REFERENCES

1. Yonesaki, T., and Minagawa, T. (1985) *EMBO J. 4*, 3321−3327.
2. Yonesaki, T., and Minagawa, T. (1989) *J. Biol. Chem. 264*, 7814−7820.
3. Morrical, S. W., and Alberts, B. M. (1990) *J. Biol. Chem 265*, 15096−15103.
4. Kodadek, T., Gan, D.-C., and Stemke-Hale, K. (1989) *J. Biol. Chem. 264*, 16451−16457.
5. Hinton, D., and Nossal, N. (1986) *J. Biol. Chem. 261*, 5663−5673.
6. Harris, L. D., and Griffith, J. D. (1989) *J. Mol. Biol. 206*, 19−28.
7. Griffith, J., and Formosa, T. (1985) *J. Biol. Chem. 260*, 4484−4491.
8. Formosa, T., and Alberts, B. (1986) *J. Biol. Chem. 261*, 6107−6118.
9. Formosa, T., and Alberts, B. (1986) *Cell 47*, 793−806.
10. Jiang, H., Salinas, F., and Kodadek, T. (1997) *Biochem. Biophys. Res. Commun. 231*, 600−605.
11. Beernink, H. T. H., and Morrical, S. W. (1998) *Biochemistry 37*, 5673−5681.
12. Kowalczykowski, S. C., Lonberg, N., Newport, J. W., and von Hippel, P. H. (1981) *J. Mol. Biol. 145*, 75−104.
13. Formosa, T., and Alberts, B. M. (1984) *Cold Spring Harbor Symp. Quant. Biol. 49*, 363−370.
14. Formosa, T., Burke, R., and Alberts, B. M. (1983) *Proc. Natl. Acad. Sci. U.S.A. 80*, 2442−2446.
15. Kodadek, T. (1990) *Biochem. Biophys. Res. Commun. 172*, 804−810.
16. Yassa, D. S., Chou, K.-M., and Morrical, S. W. (1997) *Biochimie 79*, 275−282.
17. Ando, R. A., and Morrical, S. W. (1998) *J. Mol. Biol. 283*, 785−796.
18. Jiang, H., Giedroc, D., and Kodadek, T. (1993) *J. Biol. Chem. 268*, 7904−7911.
19. Cunningham, R. P., and Berger, H. (1977) *Virology 80*, 67−82.
20. Melamede, R. J., and Wallace, S. S. (1977) *J. Virol. 24*, 28−40.
21. Melamede, R. J., and Wallace, S. S. (1978) *FEBS Lett. 87*, 12−16.
22. Melamede, R. J., and Wallace, S. S. (1980) *Mol. Gen. Genet. 177*, 501−509.
23. Sweezy, M. A., and Morrical, S. W. (1997) *J. Mol. Biol. 266*, 927−938.
24. Williams, K. R., and Konigsberg, W. H. (1983) in *Bacteriophage T4* (Mathews, C. K., Kutter, E. M., Mosig, G., and Berget, P. B., Eds.) pp 82−89, American Society for Microbiology, Washington, DC.
25. Hurley, J. M., Chervitz, S. A., Jarvis, T. C., Singer, B. S., and Gold, L. (1993) *J. Mol. Biol. 229*, 398−418.
26. Morrical, S. W., Hempstead, K., and Morrical, M. D. (1994) *J. Biol. Chem. 269*, 33069−33081.
27. Giedroc, D., Giu, H., Khan, R., King, G., and Chen, K. (1992) *Biochemistry 31*, 765−774.
28. Gill, S. C., and von Hippel, P. H. (1989) *Anal. Biochem. 182*, 319−326.
29. Miller, H. (1987) *Methods Enzymol. 152*, 145−170.
30. Menetski, J. P., and Kowalczykowski, S. C. (1985) *J. Mol. Biol. 181*, 281−295.
31. Ames, B. N. (1966) *Methods Enzymol. 8*, 115−118.
32. Alberts, B. M., and Herrick, G. (1971) *Methods Enzymol. 22*, 198−217.
33. Jensen, D., Kelly, R., and von Hippel, P. H. (1976) *J. Biol. Chem. 251*, 7215−7228.
34. Delius, H., Mantell, N., and Alberts, B. M. (1972) *J. Mol. Biol. 67*, 341−350.
35. Newport, J. W., Lonberg, N., Kowalczykowski, S. C., and von Hippel, P. H. (1981) *J. Mol. Biol. 145*, 105−121.
36. Kowalczykowski, S. C. (1990) in *Numerical data and functional relationships in science and technology* (Saenger, W., Ed.) pp 244−263, Springer-Verlag, Berlin.
37. Cowan, J., D'Acci, K., Guttman, B., and Kutter, E. (1994) in *Molecular Biology of Bacteriophage T4* (Karam, J. D., and Drake, J. W., Eds.) p 520, American Society for Microbiology, Washington, DC.
38. Shan, Q., Bork, J., Webb, B., Inman, R., and Cox, M. (1997) *J. Mol. Biol. 265*, 519−540.
39. Umezu, K., Chi, N. W., and Kolodner, R. D. (1993) *Proc. Natl. Acad. Sci. U.S.A. 90*, 3875−3879.
40. Umezu, K., and Kolodner, R. D. (1994) *J. Biol. Chem. 269*, 30005−30013.
41. Shinohara, A., and Ogawa, T. (1998) *Nature 391*, 404−407.
42. Sung, P. (1997) *Genes Dev. 11*, 1111−1121.
43. Sung, P. (1997) *J. Biol. Chem. 272*, 28194−28197.
44. New, J. H., Sugiyama, T., Zaitseva, E., and Kowalczykowski, S. C. (1998) *Nature 391*, 407−410.
45. Benson, F. E., Baumann, P., and West, S. C. (1998) *Nature 391*, 401−404.
46. Firmenich, A. A., Elias-Arnanz, M., and Berg, P. (1995) *Mol. Cell Biol. 15*, 1620−1631.

BI9817055